

Washington University in St. Louis

Washington University Open Scholarship

Mechanical Engineering and Materials Science
Independent Study

Mechanical Engineering & Materials Science

4-27-2020

CFD Study of Wake Interactions from Multiple Vertical Axis Wind Turbines using Actuator Cylinder Theory

Cory Schovanec

Washington University in St. Louis

Ramesh K. Agarwal

Washington University in St. Louis

Follow this and additional works at: <https://openscholarship.wustl.edu/mems500>

Recommended Citation

Schovanec, Cory and Agarwal, Ramesh K., "CFD Study of Wake Interactions from Multiple Vertical Axis Wind Turbines using Actuator Cylinder Theory" (2020). *Mechanical Engineering and Materials Science Independent Study*. 118.

<https://openscholarship.wustl.edu/mems500/118>

This Final Report is brought to you for free and open access by the Mechanical Engineering & Materials Science at Washington University Open Scholarship. It has been accepted for inclusion in Mechanical Engineering and Materials Science Independent Study by an authorized administrator of Washington University Open Scholarship. For more information, please contact digital@wumail.wustl.edu.

E37 MEMS 500 09 Independent Study Final Report
**CFD Study of Wake Interactions from Multiple
Vertical Axis Wind Turbines using Actuator Cylinder
Theory**

Cory Schovanec¹ and Ramesh K. Agarwal ²
Washington University in St. Louis, St. Louis, MO 63130

This paper studies the flow field and power generation from Vertical Axis Wind Turbine (VAWT) arrays using an extension of the Actuator Cylinder Model that includes the viscous effects. The ideal spacing for two VAWT arrays is determined by solving the Reynolds-Averaged Navier Stokes (RANS) equations with the Spalart-Allmaras (SA) turbulence model in ANSYS Fluent. Next, a third VAWT is introduced downfield and calculations are repeated to determine the ideal downfield distance for each spacing variation of the leading row of two turbines. Comparisons are made with an isolated vertical axis wind turbine. Differences in generated power are discussed.

Nomenclature

C_D = rotor drag coefficient
 C_P = rotor power coefficient
 D = rotor diameter
 F_D = total drag force on cylinder
 Δp = pressure jump
 P = converted power
 R = rotor radius
RANS = Reynolds Averaged Navier-Stokes
 s = turbine spacing
SA = Spalart-Allmaras turbulence model
 ρ = density of air
 V_∞ = free stream velocity
 v_r = radial velocity
 v_x = x component of velocity
 x_{DF} = downfield spacing

1 Graduate Student, Dept. of Mechanical Engineering & Materials Science.

2 William Palm Professor of Engineering, Dept. of Mechanical Engineering & Materials Science

I. Introduction

The two primary classifications for wind turbines are Horizontal Axis Wind Turbines (HAWT) and Vertical Axis Wind Turbines (VAWT). In each case, the distinguishing factor is the direction of the axis of rotation relative to the direction of the wind. The axis of rotation for HAWTs is parallel to the wind while the axis of rotation for VAWTs is perpendicular to the wind. For VAWTs, a perpendicular axis of rotation provides a number of benefits; the first of which is a radially symmetric blade path. This allows VAWTs to have directional independence from the wind. VAWTs remain optimally aligned with the wind despite any directional change in the freestream velocity.

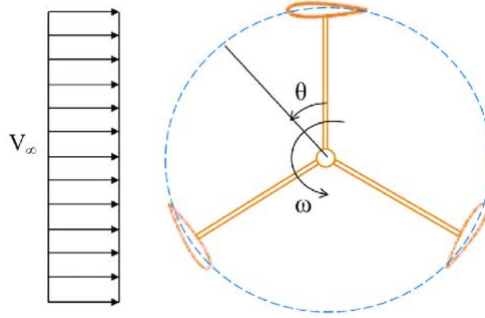


Fig. 1 Schematic of VAWT [1]

Comparatively, HAWTs require a yaw mechanism to adjust the changing direction of the wind [2]. If the blade path is not perpendicular to the wind direction, losses in efficiency can occur. This is shown below in Fig. 2.

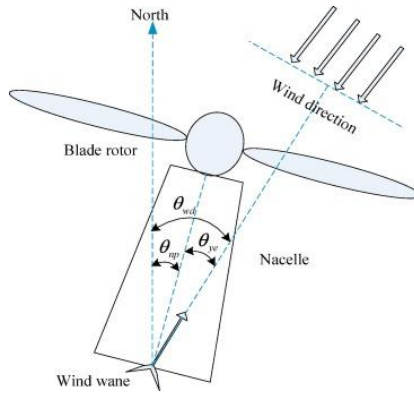


Fig. 2 Schematic of HAWT [2]

A second advantage associated with the design of VAWTs is that less land is required. HAWTs produce large wakes that can significantly affect the performance of downfield turbines. Up to 10 times the diameter of a HAWT is typically required between rows in a wind farm [3]. Despite having a lower efficiency, research has suggested that VAWTs can achieve a higher power density because they require less space between turbines than HAWTs. In fact, when properly aligned, VAWTs in an array may observe a boost in efficiency relative to isolated VAWTs [4].

The purpose of this study is to explore the optimum spacing between VAWTs and to evaluate the potential increase in efficiency that may occur. To investigate the flow behavior and power generation capabilities around VAWTs, Actuator Cylinder Theory is employed [5]. For the actuator cylinder model, an infinitely thin pressure jump boundary condition is modeled about the periphery of a thin circular cylinder. The pressure jump has the form:

$$\Delta p(\theta) = \Delta p_{max} \frac{\sin(\theta)}{|\sin(\theta)|} (1 - |\cos(\theta)|^m + \frac{1}{2\pi} \sin(2\pi |\cos(\theta)|^m)) \quad (1)$$

where Δp_{max} is the maximum pressure coefficient which is equal to the drag force over the swept area of the VAWT.

$$\Delta p_{max} = \frac{D}{2R} = \frac{1}{2} \cdot CD \cdot \rho \cdot V_{\infty}^2 \quad (2)$$

Here, the angle is defined counterclockwise relative to the positive y axis, as shown below.

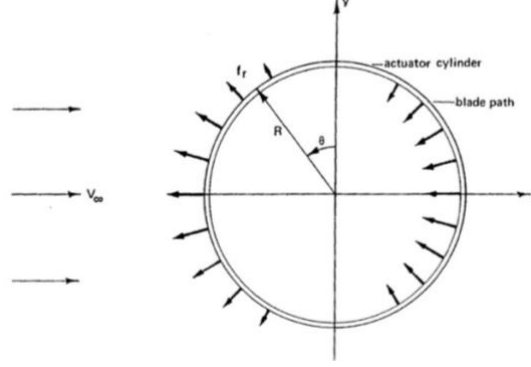


Fig. 2 Schematic of Actuator Cylinder [5]

The exponent m is a constant; as m increases the load form associated with the pressure jump becomes increasingly uniform. This results in a wider and more uniform wake profile.

To analyze the performance of the VAWT, the power per unit length of the rotor can be determined as:

$$P = \int_0^{2\pi} v_r \cdot \Delta p(\theta) \cdot R \cdot d\theta \quad (3)$$

where v_r is the radial velocity at the exterior of the cylinder. For discrete analysis, the power can be estimated using a Riemann sum as follows:

$$\sum_{i=1}^{i=n} v_{r,i} \cdot \Delta p_i \cdot R \cdot \Delta\theta \quad (4)$$

The power coefficient C_p can be then be calculated as the ratio of the calculated power to the theoretically possible power from the wind.

$$C_p = \frac{P}{\frac{1}{2} \cdot \rho \cdot V_{\infty}^3 \cdot 2R} \quad (5)$$

II. Numerical Method and Validation

A. Physical Model and Grid

In this study, two and three VAWT arrays have been created. For both cases, an actuator cylinder diameter of 2m was used with $V_{\infty} = 10$ m/s. For each spacing, m was taken to be 20; this value was selected as it represented a fully developed wake profile which spans a distance 3% wider than the diameter of each actuator cylinder.

For the two turbine cases, the actuator cylinders were directly in line with each other with the lower turbine centered about the origin. This is important because the definition of the radial velocity in Eq. 3 for the power calculation is dependent on the position relative to the coordinate axes. As such, all of the power calculations were made for the lower turbine.

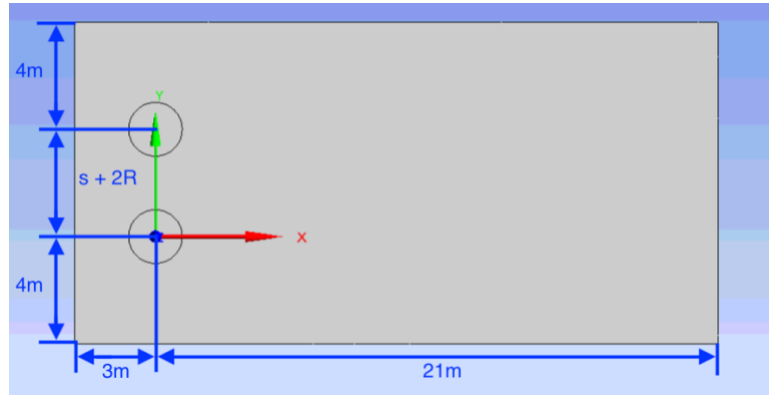


Fig. 3 Geometry for two VAWT configurations

To determine the ideal spacing, geometries were created for $s = 0.5\text{m}$, $s = 1\text{m}$, $s = 2\text{m}$, $s = 4\text{m}$, $s = 8\text{m}$, $s = 16\text{m}$, and $s = 24\text{m}$. As seen in Fig. 3, the remaining distances in the domain were constant. The distances between the front edge to the center of the actuator cylinders was 3m and the distances between the top and bottom edges to the center of the nearest actuator cylinder were 4m each. Twenty-one meters was used for the distance between the centers of the cylinders to the far field boundary.

For three VAWT arrays, an additional turbine was added directly between the leading row at a variable distance x_{DF} downstream. The remaining distances in the geometry were the same. The downfield distance was chosen to vary by increments of 0.5m ranging from an even alignment to 3.5m downstream. Here, the spacing is measured from the trailing edge of the front VAWTs to the leading edge of the downfield actuator cylinder. This is demonstrated below for a spacing of 2m and a downfield distance of 3.5m .

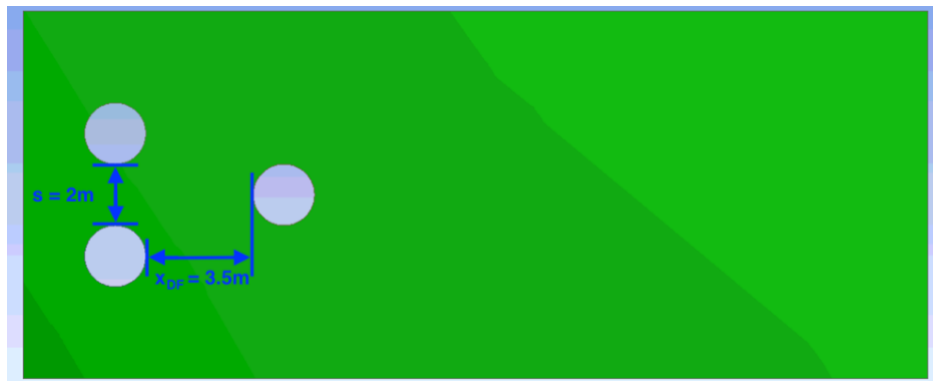


Fig. 4 Geometry for three VAWT configurations

For both the two and three VAWT cases, a hybrid mesh with inflation about the periphery of the cylinders was used. For each case, a number of mesh refinements were performed until decreasing the mesh size further had no significant bearing on the power output. This ensured grid independence of the solutions and reduced the computational intensity for each model.

B. Numerical Model

The Incompressible RANS equations were solved using the SA model for turbulence. For the boundary conditions, the left side of the computational domain is considered as a velocity inlet. The right side of the domain is considered as a pressure outlet. Both the top and bottom exterior edges of

the computational domain are modeled as far field velocity conditions with the same velocity as of the inlet. Since the entire domain was modeled as a fluid medium, the actuator cylinder zone type was double-sided. To model the pressure jump for a double-sided zone, a fan boundary condition is set around the periphery of the cylinder. In order to properly orient the fan boundary condition toward the far field outlet, the direction of the fan was reversed. A 360-point profile is created using Eq. 1 for the pressure jump of each fan in the model. The SimpleC numerical algorithm was used with convergence criteria of 10^{-5} .

III. Results and Discussion

A. Two VAWTs Analysis

Power was calculated for each combination of VAWT spacing and m . The trend in rotor power as spacing increased was plotted relative to the power of a single actuator cylinder. The following trend was found; the power for the isolated actuator cylinder is represented by the orange dotted line

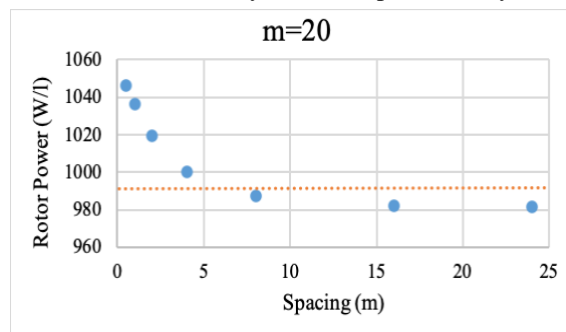


Fig. 5 Power versus spacing

As can be seen above in Fig. 31, as spacing increased the power of each actuator cylinder in the pair approached the power from the isolated case. This is a required result for the model. It can also be observed that the power output increased as $s \rightarrow 0m$. This result was due to interacting regions of increased velocity outside of the actuator cylinders' wakes. To see this trend, consider the velocity contours below in Fig. 6 (a), Fig 6 (b), Fig 6 (c).

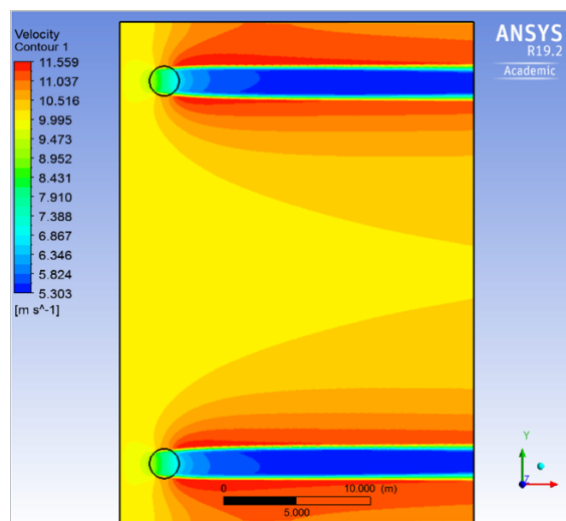


Fig. 6 (a) Velocity contours of two VAWTs with $s = 24m$

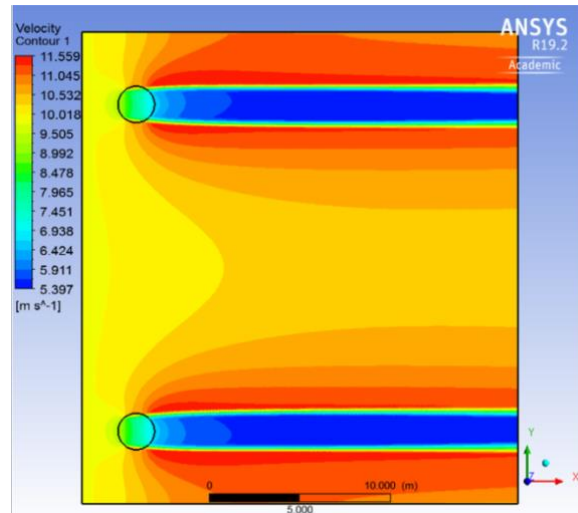


Fig. 6 (b) Velocity contours of two VAWTs with $s = 16\text{m}$

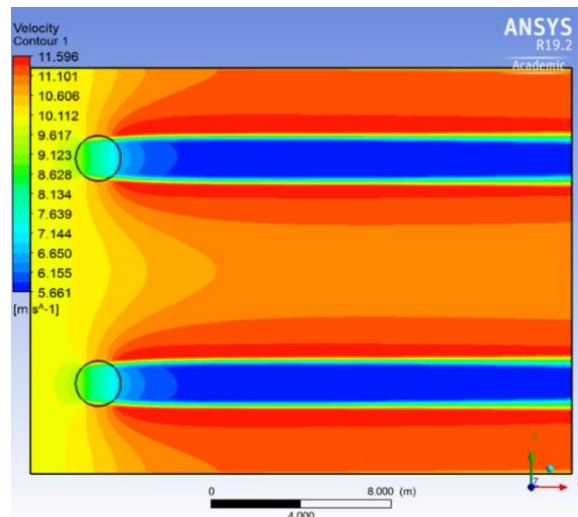


Fig. 6 (c) Velocity contours of two VAWTs with $s = 8\text{m}$

As spacing decreases, the regions of increased velocity outside of the wakes interact to result in an even higher magnitude. This effect, which demonstrates the benefits of properly aligned VAWTs, becomes more pronounced as spacing decreases.

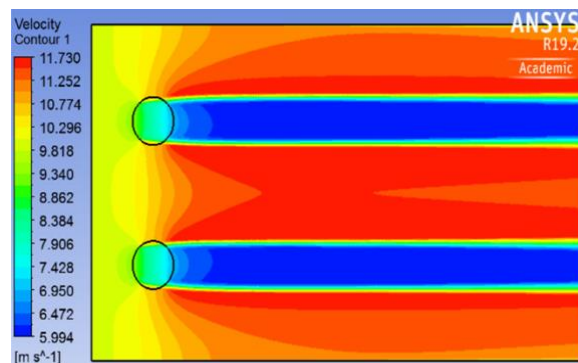


Fig. 7 (a) Velocity contours of two VAWTs with $s = 4\text{m}$

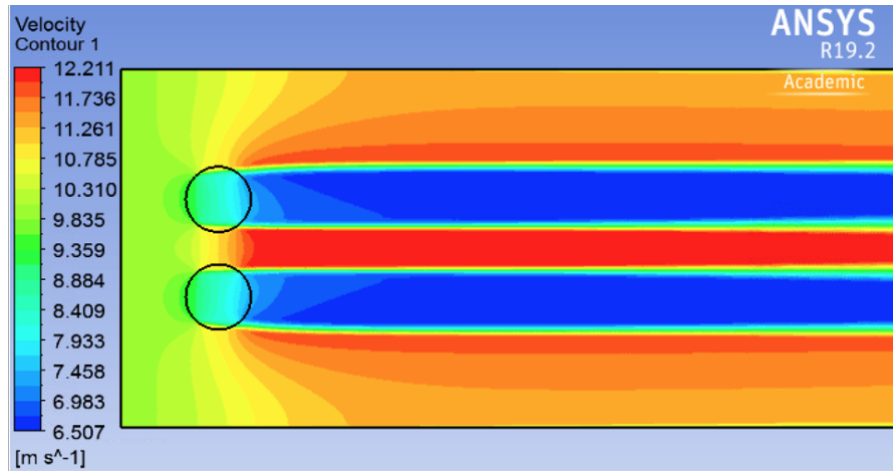


Fig. 7 (b) Velocity contours of two VAWTs with $s = 2m$

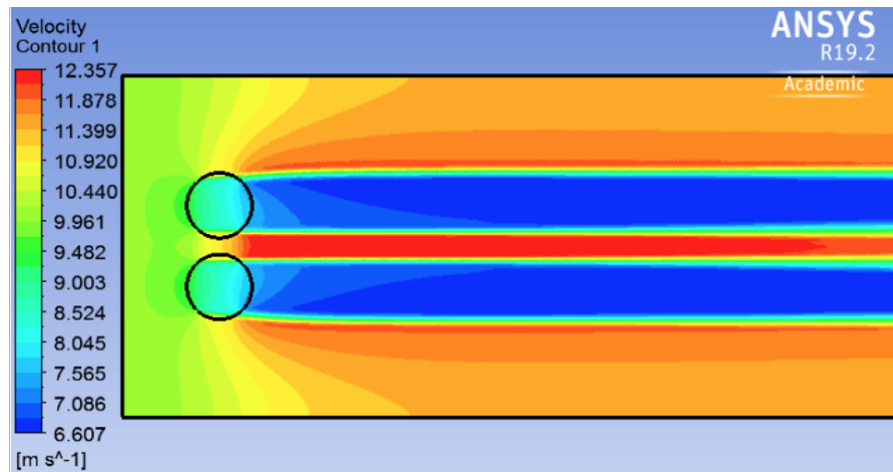


Fig. 7 (c) Velocity contours of two VAWTs with $s = 0.5m$

Power calculations for each spacing variation are shown in Table 1.

Table 1 Series of mesh refinements with number of elements

Spacing	Isolated	0.5m	1m	2m	4m
Power (W/l)	991.4	1046.4	1036.1	1019.6	1000.3
Change in Power	-	5.54%	4.51%	2.84%	0.89%

As can be seen above, the application of the actuator cylinder model suggests that narrow spacing is ideal for any pair of VAWTs. Practical limitations to this model should be considered since the model results in symmetric and ideal flow conditions.

B. Three VAWTs Analysis

Power calculations for a downfield actuator cylinder were performed for spacing variations of 0.5m, 1m, 2m and 4m. As previously addressed, the position of the third actuator cylinder was defined

with respect to the trailing edge of the leading row of VAWTs and ranged from an even alignment to 3.5m downfield. The optimum downfield position was determined for each spacing.

For each case, an inverse relationship between power and downfield distance was found for every point beyond $x_{DF} = 1m$. As can be seen in Fig. 8, the behavior prior to $x_{DF} = 1m$ varied based on the spacing of the leading row.

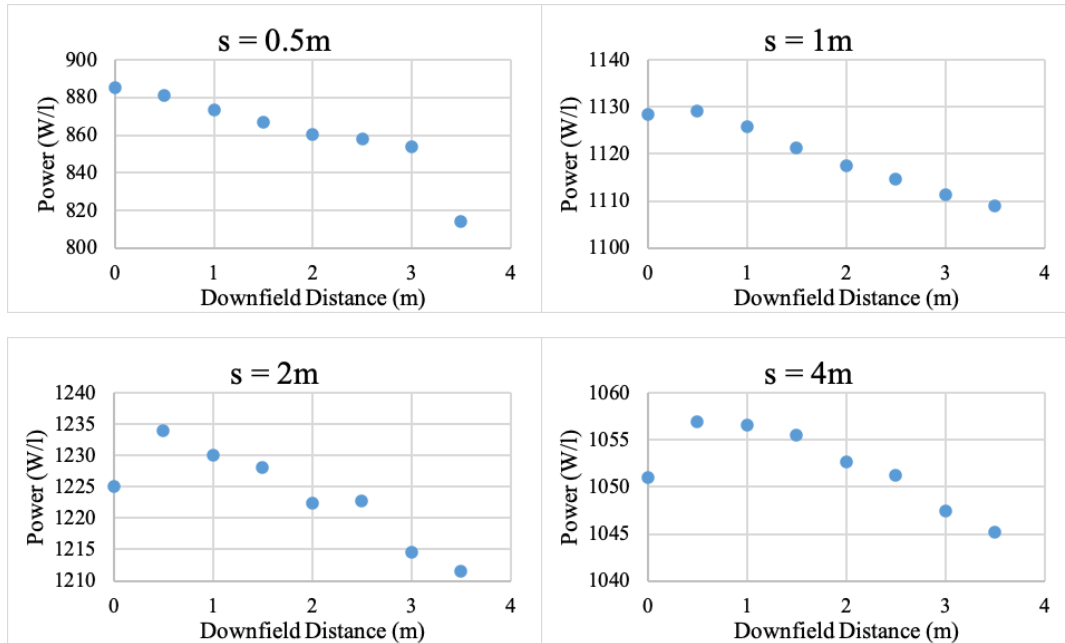


Fig. 8 Power vs downfield distance for variable spacing

For $s = 0.5m$, the maximum output was found for the case with an even alignment and decreased at every point thereafter. As spacing increased, the optimum position for the VAWT began to shift slightly downfield. For each of the remaining cases, $x_{DF} = 0.5m$ produced the highest output while the performance for the case with an even alignment decreased considerably. Narrow spacing was found to have the greatest benefit for two VAWT arrays; however, when a third VAWT was added downfield, a significant reduction in power was observed. This is shown in Fig. 9.

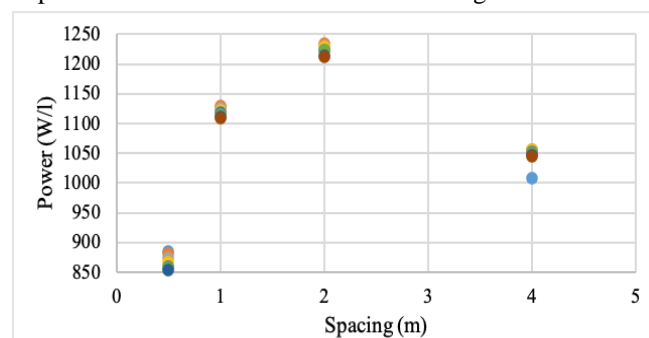


Fig. 9 Power vs leading row spacing for downfield VAWT

As can be seen above, the downfield VAWT had the lowest power for $s = 0.5m$ which is not a surprising result. As demonstrated in Fig. 30, the downfield VAWT is exposed to the wake regions of the leading row of VAWTs for cases in which the spacing is less than the diameter of the actuator cylinder. For $s = 0.5m$, half of the downfield VAWT is exposed to the wake regions of the leading row of VAWTs. This resulted in a power output for the downfield VAWT that was approximately 15.4-22.2%

lower than the power for a VAWT in a two turbine array with the same spacing.

The velocity contours for each variation in spacing are included below for a downfield distance of 0.5m.

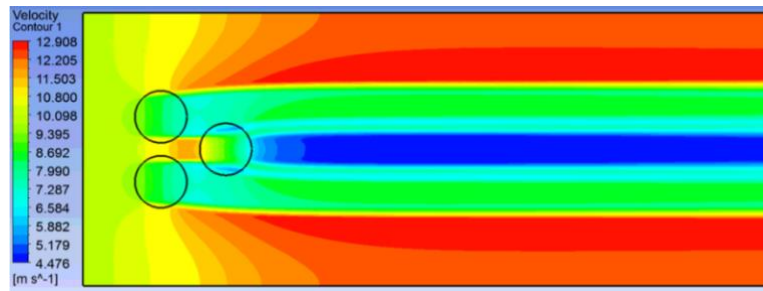


Fig. 9 (a) Velocity contour for $s = 0.5m$

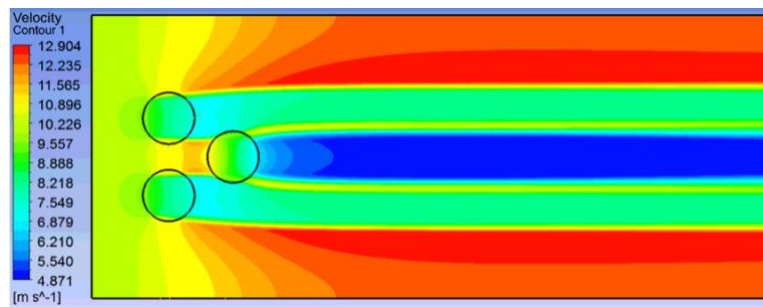


Fig. 9 (b) Velocity contour for $s = 1m$

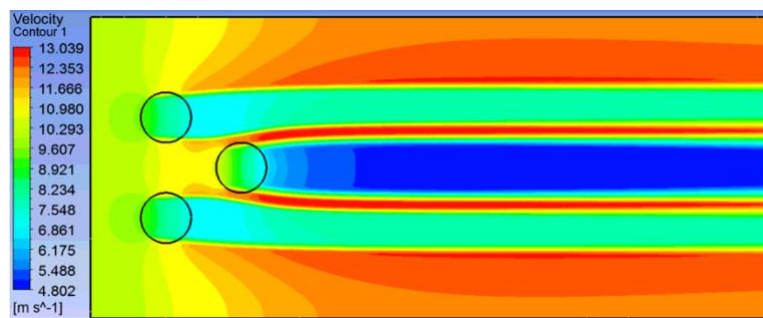


Fig. 9 (c) Velocity contour for $s = 2m$

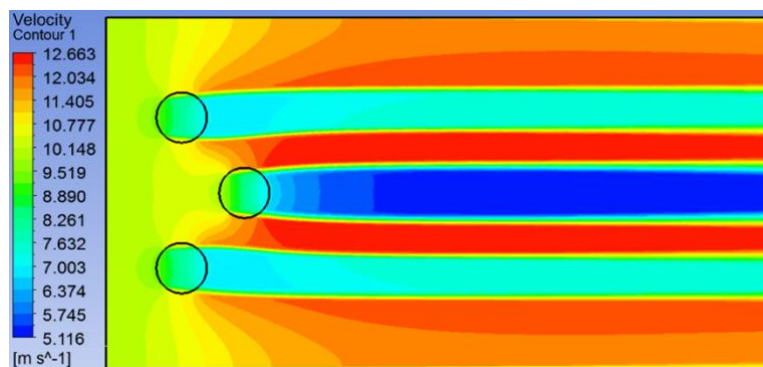


Fig. 9 (d) Velocity contour for $s = 4m$

To further optimize the power output of the downfield actuator cylinder, a series of refinement cases were performed around $s = 2m$. Trials were conducted for $s = 2.25m$, $s = 1.75m$, $s = 1.5m$, $s = 1.25m$. The results are included below in Table 2.

Table 2 Three VAWT Power Comparisons

x_{DF}	Power (W/l)							
	Even	0.5m	1m	1.5m	2m	2.5m	3m	3.5m
$s = 2.25m$	1015.8	1011.6	1009.7	1009.0	1009.1	1009.3	1009.7	1010.0
$s = 1.75m$	1189.9	1196.7	1195.6	1191.8	1187.5	1183.5	1180.1	1177.4
$s = 1.5m$	1296.0	1287.2	1271.9	1270.9	1262.3	1260.0	1261.6	1252.6
$s = 1.25m$	1234.2	1233.5	1229.0	1223.6	1218.6	1215.6	1212.2	1211.4

As can be seen above, a decrease in power occurred for $s = 2.25m$ while an increase occurred for narrower spacing up until $s = 1.25m$. This indicates that a spacing slightly less than the diameter of the downfield actuator cylinder is optimum.

IV. Conclusions

Based on this study, the following conclusions can be drawn:

- (1) Based on the Actuator Cylinder Model, narrow spacing is ideal for a two VAWT array. Compared to an isolated VAWT, the power output of an ideal VAWT in a pair can be increased by up to 5-6% due to region of elevated velocity directly outside of the wake.
- (2) Narrow spacing is detrimental to the power of a downfield VAWT. A spacing equal to $0.75D$ - $0.875D$ results in the maximum power output for the downfield VAWT.
- (3) Minor variations in power occur for the downfield VAWT as a function of downfield distance. The spacing of the leading row of VAWTs is the most influential factor regarding power output for three VAWT arrays.

V. References

- [1] Ma, N., et al, "Airfoil optimization to improve power performance of high solidity vertical axis wind turbine at a moderate tip speed ratio," *Energy*, Vol. 150, 2018, pp. 236-252.
- [2] Song, D., et al, "Maximum power extraction for wind turbines through a novel yaw control solution using predicted wind directions," *Energy Conversion and Management*, Vol. 157, 2018, pp. 587-599.
- [3] J. Meyers, C. Meneveau, "Optimal turbine spacing in fully developed wind farm boundary layers." *Wind Energy*, Vol. 15, 2012, pp. 305-317.
- [4] Hazaveh, S., et al, "Increasing the Power Production of Vertical-Axis Wind-Turbine Farms Using Synergistic Clustering," *Boundary Layer Meteorology*, Vol 169, 2018, pp. 275-296.
- [5] Madsen H., "The Actuator Cylinder: A Flow Model for Vertical Axis Wind Turbines," PhD Thesis, Aalborg University, Denmark, January 1982.